

# BEAM DYNAMICS IN SUPERCONDUCTING HIGH INTENSITY PROTON LINACS

M. Pabst, K. Bongardt, Forschungszentrum Jülich GmbH, Germany

## Abstract

Elliptical superconducting (sc) bulk Nb cavities at high frequencies will save capital and operating costs in high intensity proton linacs when used from intermediate energies on. A quite careful beam dynamical design is mandatory as frequency change and therefore increased bunch current is needed. Layout and multiparticle simulations are presented for accelerating 228 mA bunches in six cell, 1120 MHz sc cavities above 400 MeV. Energy spread reduction at 1.334 GeV can be done either by using 1120 MHz sc cavities or warm CCL structures at 560 MHz. The bottleneck is the tolerable energy resp. phase displacement at the entrance of the sc linac, but not RF errors in the sc cavities itself.

## 1 LAYOUT OF A 1120 MHz SUPERCONDUCTING (SC) LINAC

For high power proton linacs, it is a very attractive possibility to design the high energy part with elliptical sc cavities in order to reduce operating cost in cw or pulsed mode operations. High intensity  $H^-$  injector linacs for spallation neutron sources (SNS, ESS, JKI) have to deliver a chopped pulse, finally reduced in energy spread to achieve loss free ring injection. The front scheme with its chopping line prefers low frequency structures, relaxing rise time constraints on the fast chopping elements and allowing to use variable quads in the DTL [1, 2]. Elliptical sc cavities prefer higher frequencies. Therefore a possibility is to consider a frequency jump by a factor 2 or more at some intermediate energy around 400 MeV [1].

Advantages are greater peak power per coupler and therefore a reduced numbers of input couplers for the sc cavities, a smaller sc cavity size and having higher accelerating gradients. Klystrons are reduced in size and somewhat in peak power. As a consequence high frequency sc proton linacs are cheaper in capital and operating costs than low frequency sc designs. Disadvantages are the doubled bunch current and the increased sensitivity to initial phase displacements in the sc section. Envelope instabilities can occur at injection. Final energy spread reduction by bunch rotation cavities in the linac to ring transfer line have to be evaluated for initial displaced bunch centers.

In this paper, layout and multiparticle results are presented for the 280/560 MHz ESS linac scheme [3], but using 1120 MHz elliptical sc bulk Nb cavities above 400 MeV. The main data of a 1120 MHz sc linac are shown in table 1, compared with data of the  $\beta = 0.85$  sc cavities of the 350/700 MHz ESS linac [3]. We have chosen one type of cryostat with four  $\beta = 0.8$  cavities having six cells each. Transverse focusing is provided by warm doublets between the cryostats. The sc linac length is about 200 m

corresponding to 4.65 MeV/m real estate energy gain. The total length of this 1.334 GeV ESS linac is about 465 m.

Within the sc cavity the maximum accelerating gradient was chosen to be 15.5 MV/m or less than 45 MV/m peak surface gradient and the cavity mid-phase ('synchronous phase') was set to  $-25^\circ$ . Thus the maximum energy gain is 8.75 MeV per cavity corresponding to a nominal peak power less or equal to 1 MW per cavity for 114 mA pulse current. No power splitting is necessary here. Input couplers with 1.2 MW peak power and up to 3 msec pulse length requires increased RF window diameter as foreseen for the TESLA-800 design [4].

To limit dynamic RF amplitudes and phase errors to less than  $\pm 1\%$  resp.  $\pm 1^\circ$  for the ESS 50 Hz pulse scheme needs cavity stiffening either by fixing rings or by 4 mm wall thickness and enhanced axial cavity support of about 50 kN/mm [1]. An aperture radius of 4 cm will lead to more than  $\pm 1$  kHz cavity bandwidth, by a factor 2 larger than the frequency change due to Lorentz force detuning. Furthermore, the frequency shift can be counteracted by fast piezo-elements incorporated in the tuning system [4, 8]. No particle loss is expected at the 400 MeV transition point from the warm 560 MHz CCL to the sc section.

Table 1: ESS sc high  $\beta$  section: 1120 MHz vs. 700 MHz

	1120 MHz	700 MHz
Energy range	0.4-1.334 GeV	0.45-1.334 GeV
Peak pulse current	114 mA	114 mA
$\beta$ - cavity	0.8	0.85
cells/cavity	6	5
cavity length	0.64 m	0.9 m
total linac length	201 m	196 m
cavities/cryomodule	4	4
period length	7.17 m	8.52 m
nr. of cavities	112	92
nr. of klystrons	112	92
nr. of couplers	112	184
nr. of periods	28	23
accelerating gradient	15.5 MV/m	12.5 MV/m
energy gain/cavity	8.75 MeV	10.4 MeV
peak power/cavity	1.0 MW	1.2 MW
R/Q	218 $\Omega$	242 $\Omega$
Unloaded Q value	$> 5 \times 10^9$	$5 \times 10^9$
diss. peak power/m	$< 141$ W/m	116 W/m
av. diss. power/cav.	7.5 W	8.7 W
static heat load/cav.	3 W	7.5 W
matched 3 db bandw.	$\pm 1190$ Hz	$\pm 810$ Hz

## 2 MULTIPARTICLE SIMULATIONS OF THE 228 mA, 1120 MHz SC LINAC

Based on this sc linac layout we have made a careful beam dynamical design. The major beam parameters are a pulse current of 114 mA corresponding to 228 mA bunch current. The used normalized transverse, longitudinal rms emittances are  $0.27\pi$  mm mrad resp.  $0.75\pi^0$  MeV (1120 MHz), which are the 400 MeV values of the 280/560 MHz ESS linac layout. For the chosen accelerating field, the longitudinal zero current tune is  $86^\circ$  at 400 MeV, avoiding the onset of envelope instabilities [7]. The transverse full current current is set to be  $45^\circ$  all along the linac. The tune depressions are above 0.55 and the transverse/ longitudinal temperature ratio varies 0.3 and 1.3. The maximum phase slip at beginning and end the sc linac is  $110^\circ$  for 6 cell cavities.

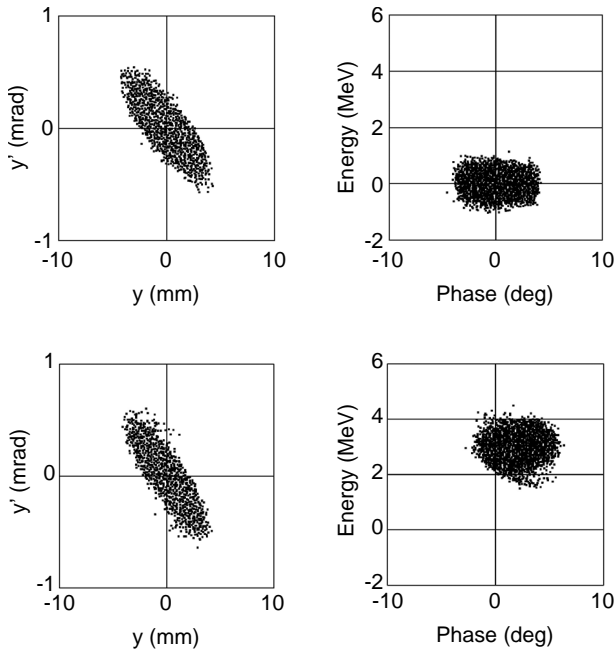


Figure 1: Horizontal and longitudinal phase space distributions at 1.334 GeV. Top: 'control' beam, Bottom: beam with RF errors and 1.3 MeV initial displacement

The top plots in Figure 1 show the resulting horizontal resp. longitudinal phase space distributions at the linac end for a matched 6d waterbag distribution with 10000 macroparticles, injected into an error free linac. Almost no transverse filamentation is caused by the 6 cell sc cavities for this 'control' beam, whereas moderate filamentations due to the large phase slip are visible in the longitudinal phase space. Fully 3d space charge forces are applied for the 228 mA bunched beam. Energy and velocity of each individual particle are changed once in the middle of each sc cell by a kick corresponding to a sinusoidal axial field distribution.

Initial energy resp. phase displacements of the particle distribution will lead to synchrotron oscillation of the

bunch center along the linac, modified by RF errors in the sc cavities.

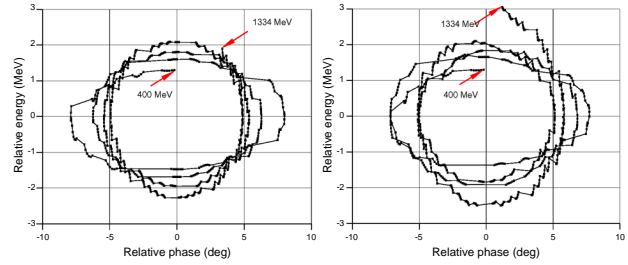


Figure 2: Synchrotron oscillation along the sc linac for initial +1.3 MeV displacement. Left: no RF errors, Right: with RF errors

Figure 2 shows the synchrotron oscillation of an initial by 1.3 MeV displaced bunch center injected into the sc linac with and without RF errors. Clearly the phase slip effects in the 6 cell cavities is visible. The resulting maximum values are  $8^\circ$  resp. 2 MeV. Applying uniform and independently distributed RF errors of  $\pm 1\%$  resp.  $\pm 1^\circ$  from cavity to cavity, one selected case is also shown in Figure 2 leading to + 3 MeV energy shift at the linac end.

Figure 3 shows the resulting shift in energy and phase of the bunch center for 5000 errors runs ( $\pm 1\%$  resp.  $\pm 1^\circ$ ) each with with three initial bunch displacements: No initial bunch displacement (black dots), + 1.3 MeV initial energy displacement (red dots) and  $4^\circ$  initial phase displacement (blue dots). Obvious is the shift of the error distribution towards larger values in energy and phase. The elliptical error boundary represents maximum values of 3 MeV resp.  $6^\circ$ . RF errors only will lead to  $\pm 2$  MeV energy spread.

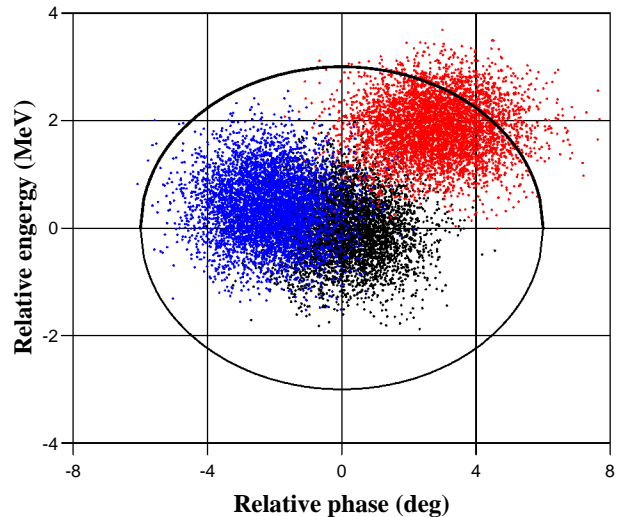


Figure 3: Scatter plot at 1.334 GeV due RF errors. Black dots: RF errors only, Red, blue dots: +1.3 MeV,  $+4^\circ$  initial displacement

The bottom plots in Figure 1 show the phase space distributions for a beam initial displaced by 1.3 MeV and one

selected case of RF errors. It leads to 3 MeV energy shift at the linac end, see Figure 2 also. Filamentation due to mismatch is obvious also in the horizontal plane. For a high intensity beam RF field errors will excite all three bunched beam eigenmodes [5, 6]. Particles have more than 4 MeV energy deviation from the linac design value. As initial energy and phase displacement are caused by RF errors in the preceding 280/560 MHz structures up to 400 MeV, consequences for energy spread reduction by bunch rotation cavities are discussed below.

### 3 ENERGY SPREAD REDUCTION AND RAMPING IN THE LINAC TO RING TRANSFER LINE

Energy spread reduction by bunch rotation cavities in the linac to ring transfer line is a common feature of spallation neutron sources. By keeping the beam focused transversely the rms phase width of the 'control' bunches is increased from  $2^\circ$  to about  $9^\circ$  along a 57 m straight line, see Figure 4. The rms energy spread is increased by more than a factor 2 due to the 228 mA bunch current. Energy spread reduction is achieved by using two  $\beta = 0.8$  1120 MHz sc cavities as before. After the bunch rotation system the total energy spread is limited to  $\pm 1$  MeV for the next 80 m, see Figure 5. Space charge forces are still visible. The 'control' bunch is slightly over-kicked behind the sc cavities.

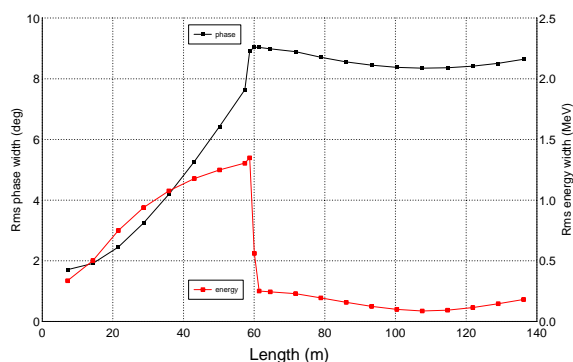


Figure 4: Rms phase width and energy spread along the linac to ring transferline

Initial energy/phase displacement at 400 MeV together with RF errors along the sc linac will lead to an elliptical error boundary of at least 3 MeV resp.  $6^\circ$  at the linac end, see Figure 3. In Figure 5 beside the 'control' bunch three bunches from the error boundary at 1.334 GeV are shown. Green dots represent a bunch displaced by 3 MeV, red dots correspond to  $6^\circ$  and blue dots to  $-2$  MeV and  $-4^\circ$  displacement. For all three cases the filamented longitudinal phase space distribution of Figure 1 is used. The left plot is directly after the bunch rotation cavities whereas the right plot is 80 m afterwards. The distributions are artificially centered in phase. RF amplitude and phase errors in the bunch rotation cavities will cause additional  $\pm 0.1$  MeV energy jitter.

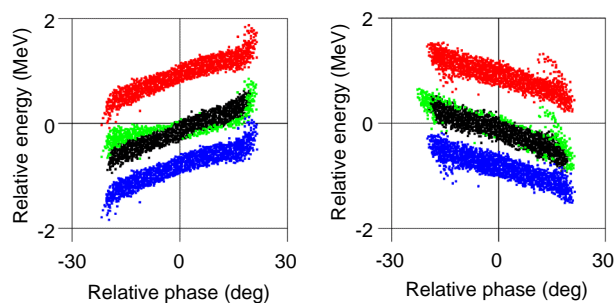


Figure 5: Energy spread reduction by sc bunch rotation cavities. Black dots: 'control' bunch, Green, red, blue dots:  $+3$  MeV,  $+6^\circ$ ,  $-2$  MeV &  $-4^\circ$  displacement at linac end

There are less than  $10^{-4}$  particles outside  $\pm 2$  MeV all along the 80 m transferline after the bunch rotation cavities, if the in Figure 3 shown error boundary contains more than 99.9% of the cases of the displaced bunch center at the linac end. As pointed out before the bottleneck is the tolerable displacements of only 1.3 MeV resp.  $4^\circ$  at 400 MeV entrance point of the sc linac and not the RF errors itself. By using warm  $\beta = 0.912$ , 560 MHz CCL structures as bunch rotation cavities, placed about 114 m behind the sc linac, beam center displacements up to 3 MeV resp.  $9^\circ$  at 400 MeV can be tolerated. There will less than  $10^{-4}$  particles outside  $\pm 2$  MeV after bunch rotation.

Loss free injection into both 1.334 GeV ESS accumulator rings requires to have less than  $10^{-4}$  particles outside  $\pm 2$  MeV at the stripping foil for each specified beam energy. In order to improve the 0.5 msec or 600 turn/ring longitudinal painting scheme, the mean beam energy has to be ramped by 6 MeV in total. Positioning a warm 560 MHz cavity directly behind the sc linac will allow to ramp the linac energy by 6 MeV during each 0.5 msec long pulse. Detailed studies are necessary to achieve with sc cavities: 6 MeV ramping in 0.5 msec for the first ESS ring, reset in 0.2 msec and 6 MeV ramping for the second ESS ring.

### REFERENCES

- [1] JAERI/KEK Joint Project, Accelerator Technical Design Report, April 2002
- [2] K. Yoshino et al., Proc. LINAC 2000, Monterrey, USA, p.569
- [3] The ESS Project, Vol. III : Technical Report, May 2002, <http://essnts.ess.kfa-juelich.de/TheESSProject>
- [4] TESLA Technical Design Report, DESY 2001-011, March 2001, [http://tesla.desy.de/new\\_pages/TDR\\_CD/start.html](http://tesla.desy.de/new_pages/TDR_CD/start.html)
- [5] K. Bongardt et al., Proc. EPAC 2000, Vienna, Austria, p. 915
- [6] A. Letchford et al., Proc. PAC 1999, New York, USA, p. 1767
- [7] M. Pabst et al., Proc. EPAC 1998, Stockholm, Sweden, p. 146
- [8] W. Bräutigam et al., Proc. PAC 1999, New York, USA, p. 1080